Dalton Transactions

Constrained geometry scandium permethylindenyl complexes for the ring-opening polymerisation of *L*- and *rac*-lactide

Received 00th January 20xx,
Accepted 00th January 20xx

DOI: 10.1039/x0xx00000x

Nichabhat Diteepeng, Jean-Charles Buffet, Zoë R. Turner and Dermot O'Hare*

The synthesis and characterisation of constrained geometry scandium permethylindenyl chloride, aryloxide and borohydride complexes ^{Me_2}SB($^{t\text{Bu}}$N,I*)Sc(Cl)(THF) (**1**), ^{Me_2}SB($^{t\text{Bu}}$N,I*)Sc(O-2,6-^{i}Pr-C$_6$H$_3$)(THF) (**2**), ^{Me_2}SB($^{t\text{Bu}}$N,I*)Sc(O-2,4-^{t}Bu-C$_6$H$_3$)(THF) (**3**) and ^{Me_2}SB($^{t\text{Bu}}$N,I*)Sc(BH$_4$)(THF) (**4**) are reported. The activity of complexes **1–4** as initiators for the ring-opening polymerisation (ROP) of *L*- and *rac*-lactide is presented. The ROP of *L*- and *rac*-lactide using complexes **2** and **3** show first-order dependence on monomer concentration, and produced isotactic polylactide (PLA) and moderate heterotactic PLA (P_r = 0.68–0.72), respectively. Good agreement between experimental and theoretical molecular weights of PLA (M_n) and relatively narrow dispersities (M_w/M_n < 1.20) were obtained. Complex **4** showed higher activity for ROP of *L*- and *rac*-lactide than **2** or **3**, with second-order dependence on monomer concentrations. However, poorly controlled molecular weights and negligible heteroselectivity (P_r = 0.61–0.67) were observed. The effect of temperature and catalyst concentration for the ROP of *L*-lactide using **2** and **3** was also studied.

Introduction

Aliphatic polyesters derived from renewable resources have gained attention as alternatives for current petroleum-based plastics.[1] Due to their mechanical and physical properties and their biodegradability and biocompatibility, potential applications of aliphatic polyesters are diverse such as single-use packaging, medical sutures and drug-delivery.[2] Ring-opening polymerisation (ROP) of cyclic esters forms well-controlled aliphatic polyesters in terms of molecular weight, composition and microstructure when using suitable initiators.[3] Group 3 metal (Sc and Y) complexes have been reported as initiators for the ROP of cyclic esters. In particular, yttrium complexes have been shown to demonstrate high activity and good polymerisation control.[4] Scandium complexes, on the contrary, have been less studied.[4m, 5] Okuda *et al.* reported the use of scandium amido complexes with bis(phenolato)-type ligand in the ROP of *rac*-lactide, producing highly heterotactic PLA (P_r = 0.78–0.95).[5b] A series of Group 3 (Sc, Y and La) amido complexes supported by a thiophene-linked bis(naphtholate) ligand afforded PLA with a decrease in heterotacticity with increasing ionic radius (metal (P_r): Sc (0.93); Y (0.84); La (0.50)).[5c] Another example of scandium amido complexes supported by amino-bridged bis(phenolate) ligands was reported by Carpentier and co-workers.[5d] Lower activity but better stereoselectivity in the ROP of *rac*-lactide initiated by scandium catalysts were observed compared to analogous yttrium complexes, rationalised by a more sterically crowded coordination sphere in scandium than yttrium. An example of scandium alkoxide complex supported by the phosphasalen ligand was reported to be inactive for the ROP of *rac*-lactide due to the monomer-insertion product which is unable to undergo the propagation step with other lactides.[4m] Scandium aryloxide supported by pentadentate (N_2O_3) salen group was reported to polymerise *rac*-lactide giving highly heterotactic PLA (P_r = 0.85) with narrow dispersity (M_w/M_n = 1.07).[5h] Ligand-free Sc(OCHPh$_2$)$_3$·(THF) was also reported as an active catalyst for the ROP of *rac*-lactide.[5e] However, kinetics and stereoselectivity of the ROP of *rac*-lactide using ligand free scandium complex were not reported.

The presence of an *ansa*-bridge between two η^5-cyclopentadienyl-type ligands of metallocene complexes could enhance the reactivity of the metallocene system by increasing the reaction space at the metal centre due to decreased Cp-M-Cp angle in comparison to non-bridged complexes, while retaining the stability of the complex by preventing the free rotation of the rings.[6] An *ansa*-scandium hydride complex, which contains a dimethylsilylene unit (SiMe$_2$) linked between two pentamethylcyclopentadienyl (C$_5$Me$_5^-$, Cp*) ligands was used as a catalyst for the dimerisation of α-olefins and cyclisation of α-ω dienes.[7] To promote the olefin insertion, one of the Cp* ligand was replaced by an amido group to render the metal more Lewis acidic and more electron deficient.[8] Scandium hydride and alkyl constrained geometry complexes containing a linked amido-Cp* ligand reported by Bercaw *et al.* were active for the polymerisations of propylene, 1-butene and 1-pentene.[8] The indenyl ligand (C$_9$H$_7^-$, Ind, I) has been an alternative to the cyclopentadienyl ligand (C$_5$H$_5^-$, Cp).[9] The more facile indenyl ring slippage from η^5 to η^3 hapticity results in higher activity of ligand substitution reactions compared to their analogous Cp

Chemistry Research Laboratory, Department of Chemistry, University of Oxford, 12 Mansfield Road, OX1 3TA Oxford, UK. E-mail: dermot.ohare@chem.ox.ac.uk

†Electronic Supplementary Information (ESI) available: NMR spectroscopy, X-ray crystallography, MALDI-ToF mass spectrometry and polymerisation data. See DOI: 10.1039/x0xx00000x

complexes.[10] Permethylation of the indenyl ring ($C_9Me_7^-$, Ind*, I*) has been shown to afford increased complex stability compared to Cp or Ind, attributed to more steric congestion, therefore leads to higher polymerisation activity.[11] Group 4 permethylindenyl constrained geometry complexes have been developed by our research group and used as catalysts for ethylene polymerisation.[12] Recently, we reported group 4 permethylindenyl *ansa*-bridged complexes used as initiators for the ROP of *L*-, *D*- and *rac*-lactide in the presence of benzyl alcohol as co-initiator.[13] Highly heterotactic PLA (P_r = 0.75–0.81) were produced from the ROP of *rac*-lactide with narrow M_w/M_n values (1.12–1.16).

In this work, a series of *ansa*-bridged scandium permethylindenyl complexes containing chloride, aryloxide or borohydride groups was prepared, and activity of those complexes for the ROP of *L*- and *rac*-lactide was investigated.

Results and Discussion

Synthesis and structural studies

Ind*SiMe$_2$Cl, proligand $^{Me}_2$SB(^{tBu}N,I*)H$_2$ and dilithium salt, $^{Me}_2$SB(^{tBu}N,I*)Li$_2$(THF)$_x$, were synthesised according to a published literature.[12c] Ind*SiMe$_2$Cl reacted with ^{tBu}NHLi in a 1:1 molar ratio in THF to give $^{Me}_2$SB(^{tBu}N,I*)H$_2$ as a yellow oil product (Scheme 1a). $^{Me}_2$SB(^{tBu}N,I*)Li$_2$ was generated *in situ* from dropwise addition of 2.2 equivalents of *n*-BuLi into the solution of $^{Me}_2$SB(^{tBu}N,I*)H$_2$ in THF at 5 °C, affording a yellow solid of $^{Me}_2$SB(^{tBu}N,I*)Li$_2$(THF)$_{0.25}$ in 54% yield after purification (Scheme 1a). We note the value of *x* representing the amount of THF molecules measured in $^{Me}_2$SB(^{tBu}N,I*)Li$_2$(THF)$_x$ can be calculated from the ^{1}H NMR spectrum of $^{Me}_2$SB(^{tBu}N,I*)Li$_2$(THF)$_x$ (Fig. S1).

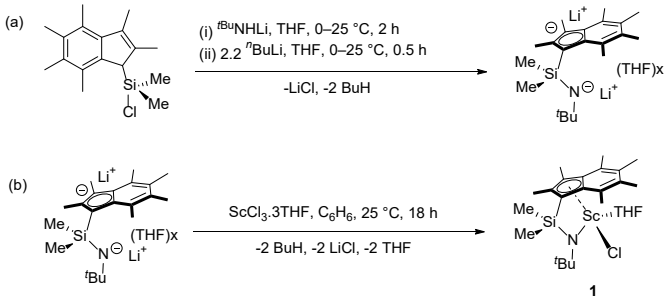

Scheme 1 Synthesis of [$^{Me}_2$SB(^{tBu}N,I*)][Li]$_2$(THF)$_x$ and $^{Me}_2$SB(^{tBu}N,I*)Sc(Cl)(THF) (**1**).

$^{Me}_2$SB(^{tBu}N,I*)Sc(Cl)(THF) (**1**) was prepared in 82% isolated yield *via* the salt elimination reaction of [$^{Me}_2$SB(^{tBu}N,I*)][Li]$_2$(THF)$_x$ and $ScCl_3$·3THF in benzene at room temperature (Scheme 1b). The ^{1}H NMR spectrum of complex **1** (Fig. S2) shows resonances of methyl protons of Ind* in the range of 1.95–2.84 ppm and those of ^{tBu}N at 1.35 ppm. Two singlets at 0.75 and 0.94 ppm define the SiMe$_2$ protons. The signals of methylene protons of a THF molecule coordinated to the metal centre were also observed.

Scandium aryloxide complexes, $^{Me}_2$SB(^{tBu}N,I*)Sc(O-2,6-^{i}Pr-C$_6$H$_3$)(THF) (**2**) and $^{Me}_2$SB(^{tBu}N,I*)Sc(O-2,4-^{t}Bu-C$_6$H$_3$)(THF) (**3**) were synthesised *via* a salt elimination reaction of **1** with KO-2,6-^{i}Pr-C$_6$H$_3$ or KO-2,4-^{t}Bu-C$_6$H$_3$ in a 1:1 molar ratio in benzene at room temperature (Schemes 2a and 2b respectively). Complexes **2** and **3** were isolated as pale-yellow and white solids in 75 and 40% respectively. The ^{1}H NMR spectra of **2** and **3** (Fig. S4 and S7) show five singlets corresponding to the indenyl methyl protons at 2.83–2.02 ppm and two singlets corresponding to the silylmethyl groups between 1.01–0.82 ppm. Multiplets corresponding to the methylene protons of coordinated THF of **2** and **3** were observed at 3.35, 3.13 and 1.00 ppm.

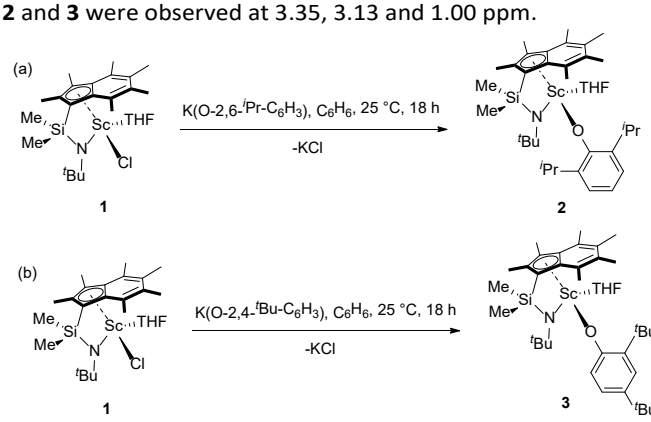

Scheme 2 Synthesis of $^{Me}_2$SB(^{tBu}N,I*)Sc(O-2,6-^{i}Pr-C$_6$H$_3$)(THF) (**2**) and $^{Me}_2$SB(^{tBu}N,I*)Sc(O-2,4-^{t}Bu-C$_6$H$_3$)(THF) (**3**).

Diffraction-quality crystals of **2** and **3** were grown *via* slow evaporation in benzene at room temperature. The molecular structures and selected distances and angles are shown in Fig. 1 and 2, and Table 1. The solid-state structures of **2** and **3** show a distorted tetrahedral geometry at the metal centre. The Sc-Cp$_{cent}$ bond length of **3** (2.1768(1) Å) is slightly longer than **2** (2.1718(1) Å) due to the increased steric bulk of the *tert*-butyl group *vs.* the isopropyl group. The absence of *tert*-butyl group at the 6-C$_6$H$_3$ (ortho) position on the phenyl ring of **3** attributes to the smaller Sc-O-C bond angle (152.93(11)°) and the shorter Sc-O (1.9324(1) Å) and Sc-N (2.0546(1) Å) bond lengths in comparison to those of **2** (175.63(9)°, 1.9450(9) and 2.0593(11) Å, respectively). To compare with the previously reported group 4 permethylindenyl complexes, the Sc-O-C bond angle and the Sc-O bond length of **2** are comparable to the Zr-O-C bond angle and the Zr-O bond length of *Z*-$^{Me}_2$SB(Cp,I*)ZrCl(O-2,6-Me-C$_6$H$_3$) (173.09(12)° and 1.9628(12) Å).[13]

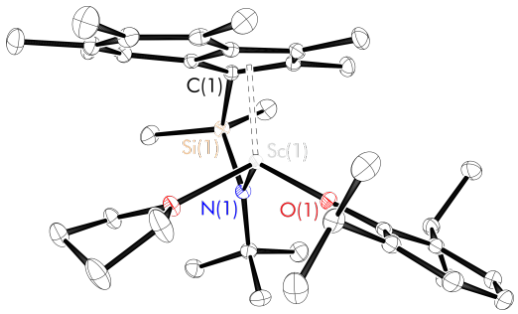

Fig. 1 Solid-state structure of $^{Me}_2$SB(^{tBu}N,I*)Sc(O-2,6-^{i}Pr-C$_6$H$_3$)(THF) (**2**). Ellipsoids are drawn at the 30% probability level. H atoms omitted for clarity.

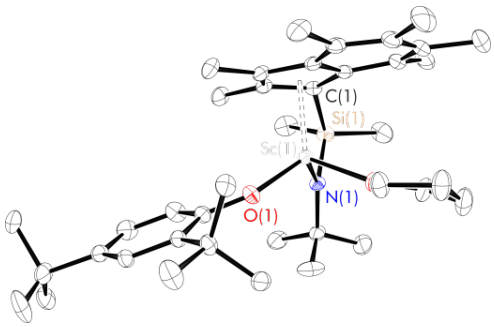

Fig. 2 Solid-state structure of ^{Me}$_2$SB(^{tBu}N,I*)Sc(O-2,4-^{t}Bu-C$_6$H$_3$)(THF) (**3**). Ellipsoids are drawn at the 30% probability level. H atoms omitted for clarity.

^{Me}$_2$SB(^{tBu}N,I*)Sc(BH$_4$)(THF) (**4**) was synthesised from reaction of **1** with KBH$_4$ in a 1:10 molar ratio in THF at room temperature and was afforded as pale-yellow solid in 57% yield after work-up (Scheme 3). The ^{1}H NMR spectrum of **4** (Fig. S10) shows five resonances of the indenyl protons from 1.97 to 2.72 ppm, and two resonances of the SiMe$_2$ protons at 0.78 and 0.96 ppm. Signals corresponding to a THF molecule coordinated to the metal centre were observed at 3.03 and 0.86 ppm. It is worth noting that the signals corresponding to BH$_4$ groups were not observed from the ^{1}H NMR spectrum (Fig. S10A). However, the chemical shift of the BH$_4$ moiety is observed as a broad singlet at δ = 0.47 ppm from the ^{1}H{^{11}B} NMR spectrum (Fig. S10B). The ^{11}B NMR spectrum (Fig. S12) showed a quintet at δ = -23.9 ppm ($^1J_{B-H}$ = 83 Hz).

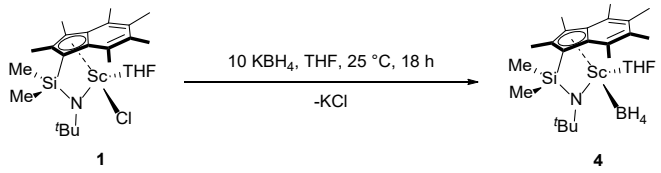

Scheme 3 Synthesis of ^{Me}$_2$SB(^{tBu}N,I*)Sc(BH$_4$)(THF) (**4**).

Crystals of **4** suitable for a single crystal X-ray diffraction study were obtained from slow evaporation in benzene at room temperature. The molecular structure of **4** is shown in Fig. 3 and the selected bond lengths and angles are shown in Table 1. Complex **4** is pseudo four-coordinate with Sc coordinated to Ind*, ^{tBu}N, THF and the BH$_4$ group coordinated in a κ^3 mode to the metal with a Sc-B distance of 2.3572(16) Å. The metal-boron bond length is in the expected range.[14] Monoborohydride or bisborohydride scandium complexes supported by amidinate or bis(phosphinimino) methanide ligands reported by Roesky *et al*. show BH$_4$ groups in κ^3 coordination mode with Sc-B bond lengths in the range 2.310–2.367 Å.[5a, 14b, 14e] The IR spectrum of **4** (Fig. S13) shows characteristic bands at 2292 and 2464 cm^{-1} assigned to terminal B-H$_t$ unit which are in agreement with the aforementioned bisborohydride scandium complex (2291 and 2495 cm^{-1}).[14b] The Sc-Cp$_{cent}$ and Sc-N bond distances of **4** (2.1631(1) and 2.0535(11) Å) are shorter than their analogue aryloxide complexes (**2** or **3**) due to the decreased steric hindrance of the BH$_4$ group. Complex **4** also shows a smaller Δ_{M-C} distance (0.0785 Å) than those from **2** (0.0892 Å) or **3** (0.0898 Å).

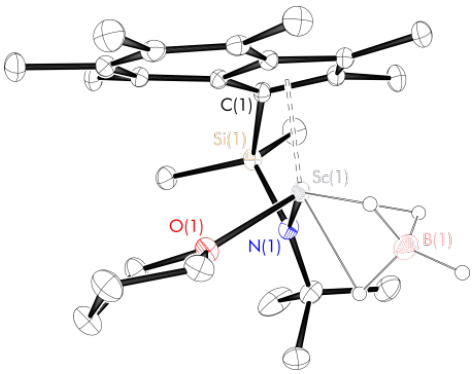

Fig. 3 Solid-state structure of ^{Me}$_2$SB(^{tBu}N,I*)Sc(BH$_4$)(THF) (**4**). Ellipsoids are drawn at the 30% probability level. H atoms omitted for clarity (excepted for BH$_4^-$ group).

Table 1 Selected bond lengths (Å) and angles (°) for ^{Me}$_2$SB(^{tBu}N,I*)Sc(O-2,6-^{i}Pr-C$_6$H$_3$)(THF) (**2**), ^{Me}$_2$SB(^{tBu}N,I*)Sc(O-2,4-^{t}Bu-C$_6$H$_3$)(THF) (**3**) and ^{Me}$_2$SB(^{tBu}N,I*)Sc(BH$_4$)(THF) (**4**). (E.S.D. are given in parentheses).

Complex	**2**	**3**	**4**
Sc-Cp$_{cent}$ (Å)	2.1718(1)	2.1768(1)	2.1631(1)
Sc-OAr (Å)	1.9450(9)	1.9324(1)	-
Sc-N (Å)	2.0593(11)	2.0546(1)	2.0535(11)
Sc-B (Å)	-	-	2.3572(16)
Sc-O-C (°)	175.63(9)	152.93(11)	-
Cp$_{cent}$-Sc-O (°)	119.70(1)	120.07(1)	-
Cp$_{cent}$-Sc-N (°)	103.99(1)	104.06(1)	104.70(1)
Δ_{M-C} (Å)	0.0892	0.0898	0.07845

Polymerisation of *L*- and *rac*-lactide studies

Complexes **1–4** were used as initiators for the ring-opening polymerisation (ROP) of *L*- and *rac*-lactide.

^{Me}$_2$SB(^{tBu}N,I*)Sc(Cl)(THF) (**1**) was initially tested as a catalyst for the polymerisation of *L*-lactide. At 70 °C with a monomer-to-catalyst ratio of 100 in benzene, more than 85% conversion of *L*-lactide was reached after 5 h (Table S3). A higher polymerisation rate was observed when benzyl alcohol was used as co-initiator with 94% conversion after 50 minutes under analogous conditions (Table S4). First-order dependence on monomer concentration was determined with k_{obs} = 3.85 and 0.40 h^{-1} for the ROP of *L*-lactide using **1** with and without benzyl alcohol, respectively (Fig. S36 and S37). Isotactic poly(*L*-lactide)s were produced and no epimerisation was observed, determined by ^{1}H{^{1}H} NMR spectroscopy (Fig. S14 and S15).

Data for polymerisation of *L*- and *rac*-lactide using ^{Me}$_2$SB(^{tBu}N,I*)Sc(O-2,6-^{i}Pr-C$_6$H$_3$)(THF) (**2**) and ^{Me}$_2$SB(^{tBu}N,I*)Sc(O-2,4-^{t}Bu-C$_6$H$_3$)(THF) (**3**) are summarised in Table 2. Experiments were carried out in benzene with initial concentration of lactide monomer [LA]$_0$ of 0.5 M and [LA]$_0$:[Sc]$_0$ ratio of 1000.

Complex **3** shows higher activity than **2** in the ROP of *L*-lactide at 70 °C. More than 90% monomer conversion was reached after 45 minutes using **3** and 4 h using **2**. Kinetics studies show a first-order dependency on *L*-lactide concentration, evidenced by linear plots of ln([*L*-LA]$_0$/[*L*-LA]$_t$) *vs.* time of polymerisation (Fig. S38 and S48) with k_{obs} = 0.66 and 8.67 h^{-1} for the polymerisation using **2** or **3**, respectively.

Table 2 Selected polymerisation data using complexes **2** and **3**.[a]

Cat.	T (°C)	LA	*t* (h)	Conv. (%)	M_n (GPC)[b]	M_n (calcd)[c]	M_w/M_n
2	70	*L*-	4	90	111160	129868	1.12
2	70	*rac*-	1	86	82380	124104	1.10
3	70	*L*-	0.75	95	84560	137101	1.19
3	50	*L*-	1	88	126400	127014	1.10
3	50	*rac*-	1.5	94	129940	135660	1.10

[a]Conditions: $[LA]_0:[Sc]_0 = 1000$, $[LA]_0 = 0.5$ M, 7.0 mL benzene. [b]Determined by GPC in chloroform at 30 °C against PS standards (M_n values are corrected by factor of 0.58).[15] [c]Calculated M_n for PLA synthesised by using **2** = conv.(%) x 1000 x 144.1 + 178.1 and calculated M_n for PLA synthesised by using **3** = conv.(%) x 1000 x 144.1 + 206.2.

Table 3 Selected polymerisation data using various concentrations of complex **2**.[a]

$[L\text{-LA}]_0:[\mathbf{2}]_0$	*t* (h)	Conv. (%)[b]	k_{obs} (h^{-1})	M_n (GPC)[c]	M_n (calcd)[d]	M_w/M_n
1000	4	90	0.66 ± 0.01	111160	129868	1.12
800	3	90	0.82 ± 0.03	87810	103930	1.12
600	3	93	1.07 ± 0.04	68220	80586	1.14
400	2.75	94	1.47 ± 0.05	56470	54359	1.17

[a]Conditions: $[L\text{-LA}]_0$ = 0.5 M, 7.0 mL benzene at 70 °C. [b]Measured by ^{1}H NMR spectroscopic analyses. [c]Determined by GPC in chloroform at 30 °C against PS standards (M_n values are corrected by factor of 0.58).[15] [d]Calculated M_n for PLA synthesised by using **2** = conv.(%) x 1000 x 144.1 + 178.1.

Good agreement between the experimental and calculated number averaged molecular weights (M_n) with narrow M_w/M_n value (1.12) of PLA obtained from using **2** suggested that all metal centres of **2** were active during polymerisation. Whereas the considerably lower than expected M_n and broader M_w/M_n value (1.19) for **3** were observed attributed to the presence of intramolecular transesterification reaction leading to chain-shortening effect.[16] The polymerisation of *L*-lactide with **3** was also carried out at 50 °C, and aliquots were collected every 7.5 minutes for 1 h. After the induction period of 30 minutes, first-order dependence on [*L*-LA] was determined with k_{obs} = 3.91 h^{-1} (Fig. S51). Better control over molecular weight of PLA was observed for the ROP conducted at 50 °C compared to 70 °C as the experimental M_n is consistent with the expected value, and the M_w/M_n value (1.10) becomes narrower. Isotactic pure poly(*L*-lactide) was formed, without epimerisation, during ROP of *L*-lactide with **3**, confirmed by a single resonance in the methine region of the homonuclear decoupled ^{1}H{^{1}H} NMR spectrum (Fig. S26).

The ROP of *rac*-lactide using **3** at 50 °C also shows a first order dependence on *rac*-lactide concentration with a similar rate to *L*-lactide (k_{obs} = 3.70 and 3.91 h^{-1} for *rac*- and *L*-lactide, respectively). An induction period of 45 minutes was observed (Fig. S52). The polymer tacticity studied by {^{1}H}^{1}H NMR spectroscopy showed that **3** produced PLAs with moderate heteroselectivity (P_r = 0.70–0.72) (Fig. S27). For **2**, the polymerisation rate of *rac*-lactide is twice as fast as those for *L*-lactide (Fig. 4) suggesting the preference of racemic linkage (k_{obs} = 2.46 and 0.66 h^{-1} for *rac*- and *L*-lactide, respectively). Moderate heterotactic PLAs with P_r = 0.68–0.71 were produced (Fig. S22). It remains unclear why the polymerisation behaviour of **2** shows significantly different rates between *L*- and *rac*-lactide polymerisation, while the similar polymerisation rates were observed between *L*- and *rac*-lactide polymerisation using **3** under analogous conditions.

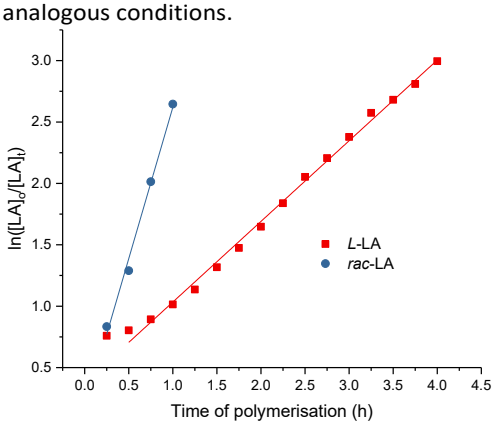

Fig. 4 Plots of $\ln([LA]_0/[LA]_t)$ *vs.* time of polymerisation. Red squares: ROP of *L*-lactide using **2**, k_{obs} = 0.66 ± 0.01 h^{-1}, R^2 = 0.996. Blue circles: ROP of *rac*-lactide using **2**, k_{obs} = 2.46 ± 0.15 h^{-1}, R^2 = 0.992. Conditions: $[LA]_0:[\mathbf{2}]_0$ = 1000, $[LA]_0$ = 0.5 M, 7.0 mL benzene at 70 °C.

It is worth noting an induction period of 5 – 45 minutes for polymerisation *L*-and *rac*-lactide using **2** and **3**. Significant induction periods have been observed for the polymerisation of cyclic esters catalysed by metal complexes with alcohol as co-initiators.[17] However, such induction periods involving metal alkoxide or aryloxide catalysts are rare. Gibson *et al.* reported the polymerisation of *rac*-lactide using tin(II) alkoxide supported by β–diketiminate ligands with induction periods from 8 – 67 minutes.[18] A slower insertion of the second (and possibly third and fourth) monomer units compared to the facile insertion of the first lactide monomer into the tin(II) alkoxide bond was reported as contributing to the induction period.

Despite similar bond distances and angles of **2** and **3**, higher *L*- and *rac*-lactide polymerisation activity of **3** than **2** could be explained by a less crowded coordination environment at the metal centre due to the less bulky aryloxide group, O-2,4-^{t}Bu-C_6H_3 of **3** *vs.* O-2,6-^{i}Pr-C_6H_3 of **2**, facilitating lactide monomer coordination to the metal centre and polymerisation by the aryloxide initiating group (Fig. S63).

To further elucidate the polymerisation behaviour of **2**, ROP of *L*-lactide with **2** using different catalyst loadings was carried out at 70 °C in benzene in order to determine the kinetic order dependence on catalyst concentration and propagation rate constant (k_p). The *L*-lactide concentration was held constant at 0.5 M, while [**2**] was varied, providing a ratio of $[L\text{-LA}]_0:[\mathbf{2}]_0$ = 1000, 800, 600 and 400. All polymerisations are summarised in Table 3. First order dependence on *L*-lactide concentration plots are shown in Fig. 5. A small induction period of 0.5 h was observed in each polymerisation. The gradient of 0.80 from the plot of $-\ln(k_{obs})$ vs. $-\ln[\mathbf{2}]_0$ is indicative of first-order dependence on concentration of **2** (Fig. 6). The propagation rate constant (k_p) of 999 M^{-1} h^{-1} was calculated from the graph between k_{obs} *vs.* $[\mathbf{2}]_0$ (Fig. 7). The overall rate law was determined as $-d[L\text{-LA}]/dt = k_p[L\text{-LA}][\mathbf{2}]$. Fair agreement between molecular weights, M_n,

determined from GPC and those predicted for one polymer chain growing per metal centre and narrow M_w/M_n (<1.2) were observed in all cases (Tables 2 and 3). These are indicators of a living ROP which implies that each metal centre generates a single PLA chain and all PLA chains are of equal length. The ^{1}H NMR spectrum of oligomers synthesised by **2** (Fig. S32) shows signals at 7.06, 6.90 and 3.16 ppm corresponding to the O-2,6-^{i}Pr-C$_6$H$_3$ end group, suggesting a coordination-insertion mechanism. The ^{1}H{^{1}H} NMR spectra of PLAs (Fig. S16–S19) show an absence of epimerisation during the ROP of *L*-lactide by **2**.

Complexes **2** and **3** display a faster rate for the ROP of lactide in comparison with those reported for scandium catalysts under similar conditions. Carpentier and co-workers reported a scandium alkyl complex supported by a phenoxy-amidopyridinate ligand with ^{i}PrOH as co-initiator in toluene at 60 °C which took 15 minutes to reach 87% conversion with [*rac*-LA]$_0$:[Sc]$_0$:[^{i}PrOH]$_0$ = 100:1:1.[5f] Only 4% conversion was achieved after 90 minutes when [*rac*-LA]$_0$:[Sc]$_0$:[^{i}PrOH]$_0$ = 500:1:1. Carpentier and co-workers also reported the use of a scandium amide complex with ^{i}PrOH as co-initiator for the ROP of *rac*-lactide in toluene at 60 °C;[5d] with [*rac*-LA]$_0$:[Sc]$_0$:[^{i}PrOH]$_0$ = 500:1:1, 74% of monomer was polymerised after 2 h. However, the PLA obtained possessed a narrow M_w/M_n (1.06) and displayed better stereocontrol with P_r = 0.82–0.75 (compared to P_r = 0.72–0.71 from **2** or **3**).The effect of temperature on *L*-lactide polymerisation activity using **2** and **3** was studied. The polymerisation temperature was varied between 50–80 °C. The enthalpy of activation ($\Delta H^‡$) and entropy of activation ($\Delta S^‡$) were calculated from an Eyring plot of ln(k_{obs}/T) *vs.* 1/T, providing $\Delta H^‡$ = 56 kJ mol^{-1} and $\Delta S^‡$ = –86 J mol^{-1} K^{-1} for **2** and $\Delta H^‡$ = 33 kJ mol^{-1} and $\Delta S^‡$ = –133 J mol^{-1} K^{-1} for **3** (Fig. 8). These values are in agreement with reported values indicating a high order in transition state in a coordination-insertion mechanism.[19]

^{Me}$_2$SB(^{tBu}N,I*)Sc(BH$_4$)(THF) (**4**) is also an efficient catalyst for the polymerisation of *L*- and *rac*-lactide. At 60 °C with [LA]$_0$:[**4**]$_0$ = 500–1000 in benzene, monomer conversions of 72–91% were attained after 15 minutes (Table 4).

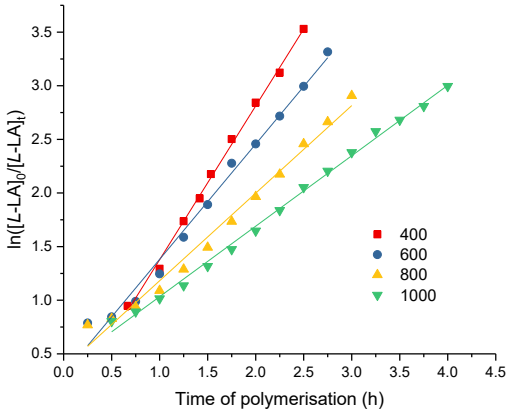

Fig. 5 Plots of ln([*L*-LA]$_o$/[*L*-LA]$_t$) *vs.* time of polymerisation. ROP of *L*-lactide using **2**. [*L*-LA]$_0$/[Sc]$_0$ = 400, red square: k_{obs} = 0.66 ± 0.01 h^{-1}, R^2 = 0.996. [*L*-LA]$_0$/[Sc]$_0$ = 600, blue circle: k_{obs} = 0.82 ± 0.03 h^{-1}, R^2 = 0.985. [*L*-LA]$_0$/[Sc]$_0$ = 800, yellow triangle: k_{obs} = 1.07 ± 0.04 h^{-1}, R^2 = 0.988. [*L*-LA]$_0$/[Sc]$_0$ = 1000, green down triangle: k_{obs} = 1.43 ± 0.03 h^{-1}, R^2 = 0.997. Conditions: [*L*-LA]$_0$ = 0.5 M, 7.0 mL benzene at 70 °C.

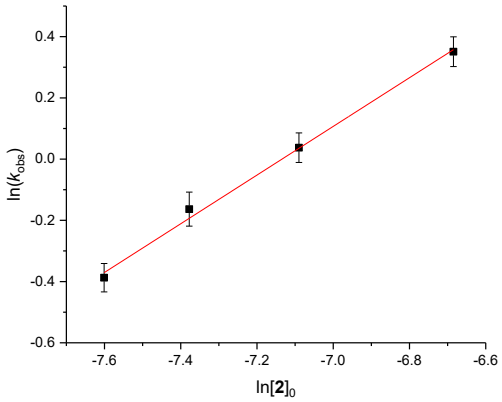

Fig. 6 Plot of ln(k_{obs}) *vs.* ln[**2**]$_0$. ROP of *L*-lactide using **2**. Slope = 0.80 ± 0.03 with R^2 = 0.997. Conditions: [*L*-LA]$_0$ = 0.5 M, 7.0 mL benzene at 70 °C. ln(k_{obs}) with standard error are calculated from two ln(k_{obs}) values over duplicate experiments.

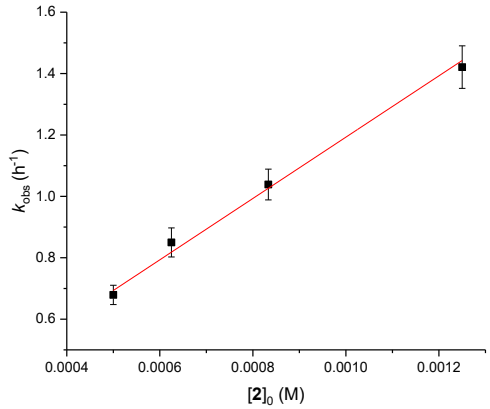

Fig. 7 Plot of k_{obs} *vs.* [**2**]$_0$. ROP of *L*-lactide using **2**. Slope = 999 ± 60 with R^2 = 0.993. Conditions: [*L*-LA]$_0$ = 0.5 M, 7.0 mL benzene at 70 °C. k_{obs} with standard error are calculated from two k_{obs} values over duplicate experiments.

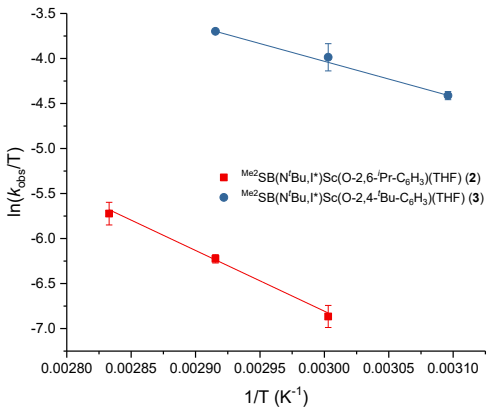

Fig. 8 Eyring plot of –ln(k_{obs}/T) *vs.* 1/T. Red square: $\Delta H^‡$ = 56 ± 5 kJ mol^{-1}, $\Delta S^‡$ = –86 ± 13 J mol^{-1} K^{-1} for ROP of *L*-lactide with **2**. Blue circle: $\Delta H^‡$ = 33 ± 1 kJ mol^{-1}, $\Delta S^‡$ = –

133 ± 2 J mol^{-1} K^{-1} for ROP of *L*-lactide with **3**. ln(k_{obs}/T) with standard error are calculated from two ln(k_{obs}/T) values over duplicate experiments.

Table 4 Selected polymerisation data using complex **4**.[a]

[LA]$_0$:[**4**]$_0$	T (°C)	LA	*t* (h)	Conv. (%)	M_n (GPC)[b]	M_n (calcd)[c]	M_w/M_n
500	60	*L*-	0.25	86	43620	61967	1.22
500	60	*rac*-	0.25	91	31260	65570	1.27
1000	60	*L*-	0.25	72	65360	103756	1.22
1000	50	*L*-	0.67	81	65930	116725	1.25
1000	50	*rac*-	0.67	91	60730	131135	1.26

[a]Conditions: [LA]$_0$ = 0.5 M, 7.0 mL benzene. [b]Determined by GPC in chloroform at 30 °C against PS standards (M_n values are corrected by factor of 0.58).[15] [c]Calculated M_n for PLA synthesised by using **4** = conv.(%) x 1000 x 144.1 + 4.

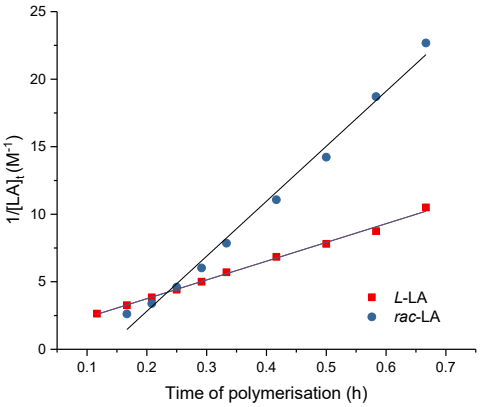

Fig. 9 Plots of 1/[LA]$_t$ *vs.* time of polymerisation. Red square: ROP of *L*-lactide using **4**, k_{obs} = 13.88 ± 0.30 M^{-1} h^{-1}, R^2 = 0.996. Blue circle: ROP of *rac*-lactide using **4**, k_{obs} = 40.70 ± 1.48 M^{-1} h^{-1}, R^2 = 0.991. Conditions: [LA]$_0$:[**4**]$_0$ = 1000, [LA]$_0$ = 0.5 M, 7.0 mL benzene at 50 °C.

Polymerisations at 50 °C with [LA]$_0$:[**4**]$_0$ = 1000 were conducted in order to gain insight into the kinetic behaviour. Polymerisation of *L*- or *rac*-lactide with **4** shows no induction period and second-order dependence on lactide concentration as determined by linear plots of 1/[LA]$_t$ *vs.* time of polymerisation; this contrasts the first-order dependence observed when using complexes **2** or **3** (Fig. 9). A second-order dependence on monomer concentration is unusual but not unprecedented. A proposed mechanism involves two lactide monomers per active site of the catalyst (Fig. S64).[20] Examples have been disclosed for the ROP of lactide promoted by group 2 and zinc,[21] lanthanum,[20] yttrium[22] or neodymium[23] catalysts. The second-order rate constant of polymerisation of *rac*-lactide (41 M^{-1} h^{-1}) is three times higher than that of *L*-lactide (14 M^{-1} h^{-1}). It is worth noting that the polymerisation mixtures formed a gel towards the end of polymerisation, causing incomplete monomer conversion especially from *L*-lactide to PLA. Similar behaviour was reported for the ROP of ε-caprolactone using borohydride catalysts.[24]

Higher polymerisation activity using **4** was found compared to the aryloxide analogues (**2** or **3**). However, there was poorer agreement between the experimental M_n and those calculated for one polymer chain per metal centre ($M_{n(GPC)}$ approximately half of $M_{n(calcd)}$) and broader M_w/M_n values (1.22–1.27) were observed (Table 4). In addition, PLAs produced from polymerisations at 50 or 60 °C show slight heterotacticity with P_r = 0.61–0.67 determined by ^{1}H{^{1}H} NMR spectroscopy (Fig. S29 and S30), lower than PLAs synthesised using **2** or **3** (0.68–0.72). These data show the effect of intermolecular transesterification occurred extensively during or after propagation, which is commonly observed for polymerisations with borohydride complexes.[5a, 14e, 24c, 25]

ROP of *rac*-lactide using **4** showed higher activity and better stereocontrol than a scandium monoborohydride catalyst supported by amidinate ligand reported by Roesky and co-workers.[5a] In this case, polymerisation of *rac*-lactide show 60-70% monomer conversion after 1 h with [*rac*-LA]$_0$:[Sc]$_0$ = 200–300 in toluene at 60 °C. Expected M_n values are half of those predicted (similar to **4**) and M_w/M_n values are in the range of 1.42-1.43. Slightly heterotactic PLAs were formed with P_r *ca.* 0.62 which is lower than those from **4**.

MALDI-ToF mass spectra of low molecular weight PLA produced by **4** (Fig. S34 and 35) show peak envelopes corresponding to α,ω-dihydroxy telechelic PLA, which implies PLA terminated with -OH and -CHMeCH$_2$OH end groups. It has been reported in the literature that BH_4^- could act as the reducing agent and initiating group in the ROP of LA or ε-caprolactone, giving polymer with a -CH$_2$OH end group by the reduction at the carbonyl carbon of monomer by two hydrides from BH_4^- ligand prior initiation.[24a, 24b, 25-26] The separation between peak envelopes by $\Delta m/z$ = 72.0 Da confirmed intermolecular transesterification. The mechanism of ring-opening polymerisation of lactide catalysed by **4** (Fig. S64) is proposed based on previous studies.[25, 27]

Conclusions

Four new scandium permethylindenyl constrained geometry complexes were synthesised, characterised and used as initiators for the polymerisation of lactide monomers.

More than 85% of *L*- or *rac*-lactide was converted, using **2** and **3**, to isotactic PLA or moderately heterotactic PLA (P_r = 0.68–0.72). All polymers display narrow M_w/M_n values (1.10–1.19) with good agreement between experimental and theoretical molecular weights. Kinetic studies for the ROP of *L*- and *rac*-lactide using **2** or **3** demonstrate first-order dependence in monomer concentrations.

Complex **4**, on the other hand, showed second-order dependence on monomer concentrations. The ROP of *L*- or *rac*-lactide by **4** is more active than those using **2** or **3** under analogous conditions. However, poor control of molecular weight (M_n) and broad polydispersities (M_w/M_n) values (1.22–1.27) were obtained due to intermolecular transesterification.

Experimental section

Synthesis of ^{Me}$_2$SB(^{tBu}N,I*)Sc(Cl)(THF) (1)

To the solid mixture of ScCl$_3$·3THF (4.62 g, 12.6 mmol) and ^{Me}$_2$SB(^{tBu}N,I*)Li$_2$(THF)$_{0.35}$ (4.38 g, 12.0 mmol) was added benzene (30 mL). The reaction mixture was stirred at room

temperature for 18 h and then the volatiles were removed *in vacuo*. Extraction into benzene followed by evaporation of the reaction mixture to dryness gave an orange solid. The solid was then washed with pentane (3 x 30 mL) to afford $^{Me}_2$SB(^{tBu}N,I*)Sc(Cl)(THF) (**1**) as a pale yellow solid (4.70 g, 82%). ^{1}H NMR (C_6D_6, 400.2 MHz, 298 K): 3.09 (4H, overlapping m, OC**H**$_2$CH$_2$), 2.84 (3H, s, Ind***Me**), 2.59 (3H, s, Ind***Me**), 2.57 (3H, s, Ind***Me**), 2.50 (3H, s, Ind***Me**), 1.96 (6H, s, Ind***Me**), 1.35 (9H, s, NC**Me**$_3$), 0.94 (3H, s, Si**Me**), 0.84 (4H, overlapping m, OCH$_2$C**H**$_2$) and 0.75 (3H, s, Si**Me**). ^{13}C{^{1}H} NMR (C_6D_6, 100.6 MHz, 298 K): 141.57 (**Ind***), 136.40 (**Ind***), 129.58 (**Ind***), 129.20 (**Ind***), 128.59 (**Ind***), 127.19 (**Ind***), 121.70 (**Ind***), 95.49 (Si-**C**Ind*), 73.08 (O**C**H$_2$CH$_2$), 54.37 (N**C**Me$_3$), 35.20 (NC**Me**$_3$), 24.90 (OCH$_2$**C**H$_2$), 22.11 (Ind***Me**), 17.21 (Ind***Me**), 16.93 (Ind***Me**), 16.14 (Ind***Me**), 15.86 (Ind***Me**), 15.62 (Ind***Me**), 11.39 (Si**Me**) and 9.08 (Si**Me**). Anal. found (calcd. for $C_{25}H_{41}ClNOScSi$): C, 62.4 (62.5); H, 8.5 (8.6); N, 2.8 (2.9)%.

Synthesis of $^{Me}_2$SB(^{tBu}N,I*)Sc(O-2,6-^{i}Pr-C$_6$H$_3$)(THF) (2)

To the solid mixture of $^{Me}_2$SB(^{tBu}N,I*)Sc(Cl)(THF) (**1**, 0.800 g, 1.67 mmol) and K(O-2,6-^{i}Pr-C$_6$H$_3$) (0.390 g, 1.83 mmol) was added benzene (30 mL). The reaction mixture was stirred at room temperature for 18 h and then the volatiles were removed *in vacuo*. Extraction into benzene followed by evaporation of the reaction mixture to dryness gave an orange solid. The resulting solid was washed with pentane (4 x 20 mL) to afford $^{Me}_2$SB(^{tBu}N,I*)Sc(O-2,6-^{i}Pr-C$_6$H$_3$)(THF) (**2**) as a pale yellow solid (0.780 g, 75%). Pale yellow crystals suitable for an X-ray diffraction study were obtained from slow evaporation of a benzene solution at room temperature. ^{1}H NMR (C_6D_6, 400.2 MHz, 298 K): 7.21 (2H, d, $^3J_{H\text{-}H}$ = 7.5 Hz, *m*-C$_6$**H**$_3$), 7.01 (1H, t, $^3J_{H\text{-}H}$ = 7.5 Hz, *p*-C$_6$**H**$_3$), 3.51 (2H, sept., $^3J_{H\text{-}H}$ = 6.8 Hz, C**H**Me$_2$), 3.35 (2H, m, OC**H**$_2$CH$_2$), 3.13 (2H, m, OC**H**$_2$CH$_2$), 2.62, 2.60, 2.53, 2.37 (3H each, s, Ind***Me**), 2.04 (6H, s, Ind***Me**), 1.37 (6H, d, $^3J_{H\text{-}H}$ = 6.8 Hz, CH**Me**$_2$), 1.30 (9H, s, NC**Me**$_3$), 1.26 (6H, d, $^3J_{H\text{-}H}$ = 6.8 Hz, CH**Me**$_2$), 1.00 (4H, overlapping m, OCH$_2$C**H**$_2$), 0.99, 0.84 (3H each, s, Si**Me**) ppm. ^{13}C{^{1}H} NMR (C_6D_6, 100.6 MHz, 298 K): 157.66, 139.33, 136.84 (**Ind***), 136.54 (**C**$_6$H$_3$), 128.73, 126.60 (**Ind***), 123.50 (*m*-**C**$_6$H$_3$), 118.98 (**Ind***), 118.55 (*p*-**C**$_6$H$_3$), 94.38 (Si-**C**Ind*), 72.70 (O**C**H$_2$CH$_2$), 54.52 (N**C**Me$_3$), 35.11 (NC**Me**$_3$), 26.04 (**C**HMe$_2$), 25.27, 25.18 (CH**Me**$_2$), 24.78 (OCH$_2$**C**H$_2$), 22.15, 17.39, 17.04, 16.19, 16.10, 14.67 (Ind***Me**), 11.56, 10.10 (Si**Me**) ppm.

Synthesis of $^{Me}_2$SB(^{tBu}N,I*)Sc(O-2,4-^{t}Bu-C$_6$H$_3$)(THF) (3)

To the solid mixture of $^{Me}_2$SB(^{tBu}N,I*)Sc(Cl)(THF) (**1**, 0.920 g, 1.92 mmol) and K(O-2,4-^{t}Bu-C$_6$H$_3$) (0.540 g, 2.11 mmol) was added benzene (30 mL). The reaction mixture was stirred at room temperature for 18 h and then the volatiles were removed *in vacuo*. Extraction into benzene followed by evaporation of the reaction mixture to dryness gave an orange solid. The resulting solid was washed with pentane to afford $^{Me}_2$SB(^{tBu}N,I*)Sc(O-2,4-^{t}Bu-C$_6$H$_3$)(THF) (**3**) as a white solid (0.500 g, 40%). Pale yellow crystals suitable for an X-ray diffraction study were obtained from slow evaporation of a benzene solution at room temperature. Assignment for aromatic protons of **3** is shown on Fig. S7. ^{1}H NMR (C_6D_6, 400.2 MHz, 298 K): 7.54 (1H, d, $^4J_{H\text{-}H}$ = 2.6 Hz, 3-C$_6$**H**$_3$), 7.34 (1H, dd, $^3J_{H\text{-}H}$ = 8.5 Hz, $^4J_{H\text{-}H}$ = 2.6 Hz, 5-C$_6$**H**$_3$), 6.96 (1H, d, $^3J_{H\text{-}H}$ = 8.3 Hz, 6-C$_6$**H**$_3$), 3.35, 3.11 (2H each, m, OC**H**$_2$CH$_2$), 2.83, 2.58, 2.53, 2.43 (3H each, s, Ind***Me**), 2.02 (6H, s, Ind***Me**), 1.57 (9H, s, 2-C**Me**$_3$-C$_6$H$_3$), 1.39 (9H, s, 4-C**Me**$_3$-C$_6$H$_3$), 1.30 (9H, s, NC**Me**$_3$), 1.05 (3H, s, Si**Me**), 0.94 (4H, m, OCH$_2$C**H**$_2$) and 0.82 (3H, s, Si**Me**) ppm. ^{13}C{^{1}H} NMR (C_6D_6, 100.6 MHz, 298 K): 160.13 (1-**C**$_6$H$_3$), 140.26 (**Ind***), 139.64 (4-**C**$_6$H$_3$), 136.66 (**Ind***), 135.16 (2-**C**$_6$H$_3$), 128.55, 128.45, 127.50, 126.60 (**Ind***), 123.88 (5-**C**$_6$H$_3$), 123.32 (3-**C**$_6$H$_3$), 123.17 (6-**C**$_6$H$_3$), 118.95 (**Ind***), 94.35 (Si-**C**Ind*), 72.73 (O**C**H$_2$CH$_2$), 54.61 (N**C**Me$_3$), 35.51 (NC**Me**$_3$), 35.39 (2-**C**Me$_3$-C$_6$H$_3$), 34.42 (4-**C**Me$_3$-C$_6$H$_3$), 32.15 (4-C**Me**$_3$-C$_6$H$_3$), 30.29 (2-C**Me**$_3$-C$_6$H$_3$), 24.75 (OCH$_2$**C**H$_2$), 22.31, 17.19, 17.02, 16.63, 16.21, 14.80 (Ind***Me**), 11.62, 9.58 (Si**Me**) ppm. Anal. found (calcd. for $C_{39}H_{62}NO_2ScSi$): C, 71.8 (72.1); H, 9.5 (9.6); N, 2.25 (2.2)%.

Synthesis of $^{Me}_2$SB(^{tBu}N,I*)Sc(BH$_4$)(THF) (4)

To the solid mixture of $^{Me}_2$SB(^{tBu}N,I*)Sc(Cl)(THF) (**1**, 0.800 g, 1.04 mmol) and KBH_4 (0.450 g, 5.20 mmol) was added THF (30 mL). The reaction mixture was stirred at room temperature for 18 h and then the volatiles were removed *in vacuo*. Extraction into benzene followed by evaporation of the reaction mixture to dryness gave an orange solid. The resulting solid was washed with pentane (4 x 20 mL) to afford $^{Me}_2$SB(^{tBu}N,I*)Sc(BH$_4$)(THF) (**4**) as a pale yellow solid (0.440 g, 57%). Pale yellow crystals suitable for an X-ray diffraction study were obtained from slow evaporation of a benzene solution at room temperature. ^{1}H NMR (C_6D_6, 400.2 MHz, 298 K): 3.03 (4H, m, OC**H**$_2$CH$_2$), 2.72, 2.60, 2.53, 2.51 (3H each, s, Ind***Me**), 1.97 (6H, s, Ind***Me**), 1.35 (9H, s, NC**Me**$_3$), 0.96 (3H, s, Si**Me**), 0.86 (4H, m, OCH$_2$C**H**$_2$), 0.78 (3H, s, Si**Me**) ppm. The resonance corresponding to B**H**$_4$ was not observed. ^{1}H{^{11}B} NMR (C_6D_6, 400.2 MHz, 298 K): 3.03 (4H, m, OC**H**$_2$CH$_2$), 2.72, 2.60, 2.54, 2.51 (3H each, s, Ind***Me**), 1.97 (6H, s, Ind***Me**), 1.35 (9H, s, NC**Me**$_3$), 0.97 (3H, s, Si**Me**), 0.85 (4H, m, OCH$_2$C**H**$_2$), 0.78 (3H, s, Si**Me**), 0.47 (4H, br s, B**H**$_4$) ppm. ^{13}C{^{1}H} NMR (C_6D_6, 100.6 MHz, 298 K): 140.38 (**Ind***), 136.83, 129.27, 128.71, 128.59, 127.03, 121.79 (**Ind***), 95.40 (Si-**C**Ind*), 73.69 (O**C**H$_2$CH$_2$), 54.25 (N**C**Me$_3$), 35.92 (NC**Me**$_3$), 25.02 (OCH$_2$**C**H$_2$), 22.28, 17.07, 17.00, 16.13, 15.97 (Ind***Me**), 11.58, 9.78 (Si**Me**) ppm. ^{11}B NMR (C_6D_6, 128.4 MHz, 298 K): -23.9 (qt, $^1J_{B\text{-}H}$ = 83 Hz, **B**H$_4$) ppm. IR (NaCl plates, Nujol mull, cm^{-1}): 2464 (s, *ν*(B-H)), 2292 (s, *ν*(B-H)), 2208 (m), 2127 (m), 1642 (m), 1287 (m), 1193 (s), 1016 (s).

General polymerisation procedure

A stock solution of catalyst (17.5 µmol) in benzene (2.5 mL) was prepared. The stock solution of catalyst (3.50 µmol, 0.5 mL) was added into a benzene solution of lactide (0.504 g, 3.50 mmol, 6.5 mL) in the ampoule, corresponding to an initial lactide concentration of 0.5 M and a monomer-to-catalyst ratio of 1000. The polymerisation ampoule was then stirred in the preheated oil bath at desired temperature. Aliquots (*ca.* 0.1 mL)

were taken at appropriate time intervals and quenched with THF (*ca.* 0.3 mL). The volatiles were evaporated to give PLA. The monomer to polymer % conversion was determined using ^{1}H NMR spectroscopy, and measured by integration of the C**H**Me resonances of the unreacted monomer and PLA. After the chosen time, the reaction was quenched with THF. The polymer was isolated by addition of pentane to a concentrated solution of PLA to yield a precipitate which was washed with pentane and dried under vacuum at 30 °C.

Conflicts of interest

There are no conflicts of interest to declare.

Acknowledgements

N.D., J.-C.B. and Z.R.T. would like to thank SCG Chemicals Co., Ltd. (Thailand) for financial support and for a SCG Research Fellowship (Z.R.T.). Dr Alexander F. R. Kilpatrick (University of Oxford) is thanked for an original synthesis of $^{Me}_{2}$SB($^{t\text{Bu}}$N,I*)Sc(Cl)(THF) (**1**). Professor Charlotte K. Williams (University of Oxford) is thanked for the use of GPC and Chemical Crystallography (University of Oxford) for the use of the diffractometers.

Notes and references

1. (a) X. Zhang, M. Fevre, G. O. Jones and R. M. Waymouth, *Chem. Rev.*, 2018, **118**, 839-885; (b) N. Mallegni, T. Phuong, M.-B. Coltelli, P. Cinelli and A. Lazzeri, *Materials*, 2018, **11**, 148.
2. (a) B. Zhang, B. Seong, V. Nguyen and D. Byun, *J. Micromech. Microeng.*, 2016, **26**, 025015; (b) H. Tian, Z. Tang, X. Zhuang, X. Chen and X. Jing, *Prog. Polym. Sci.*, 2012, **37**, 237-280; (c) J. Ahmed and S. K. Varshney, *Int. J. Food. Prop.*, 2011, **14**, 37-58.
3. (a) S. M. Guillaume, E. Kirillov, Y. Sarazin and J.-F. Carpentier, *Chem. Eur. J.*, 2015, **21**, 7988-8003; (b) C. Jérôme and P. Lecomte, *Adv. Drug Deliv. Rev.*, 2008, **60**, 1056-1076; (c) M. J. Stanford and A. P. Dove, *Chem. Soc. Rev.*, 2010, **39**, 486-494; (d) Z. Zhong, P. J. Dijkstra and J. Feijen, *J. Am. Chem. Soc.*, 2003, **125**, 11291-11298; (e) C. M. Thomas, *Chem. Soc. Rev.*, 2010, **39**, 165-173; (f) A. Sauer, A. Kapelski, C. Fliedel, S. Dagorne, M. Kol and J. Okuda, *Dalton Trans.*, 2013, **42**, 9007-9023; (g) T. M. Ovitt and G. W. Coates, *J. Am. Chem. Soc.*, 1999, **121**, 4072-4073; (h) N. Nomura, R. Ishii, M. Akakura and K. Aoi, *J. Am. Chem. Soc.*, 2002, **124**, 5938-5939; (i) P. J. Dijkstra, H. Du and J. Feijen, *Polym. Chem.*, 2011, **2**, 520-527; (j) M. H. Chisholm, J. C. Gallucci and K. Phomphrai, *Inorg. Chem.*, 2004, **43**, 6717-6725; (k) J. C. Buffet and J. Okuda, *Polym. Chem.*, 2011, **2**, 2758-2763.
4. (a) A. Amgoune, C. M. Thomas and J.-F. Carpentier, *Macromol. Rapid. Commun.*, 2007, **28**, 693-697; (b) T. V. Mahrova, G. K. Fukin, A. V. Cherkasov, A. A. Trifonov, N. Ajellal and J.-F. Carpentier, *Inorg. Chem.*, 2009, **48**, 4258-4266; (c) A. Alaaeddine, C. M. Thomas, T. Roisnel and J.-F. Carpentier, *Organometallics*, 2009, **28**, 1469-1475; (d) J.-C. Buffet, A. Kapelski and J. Okuda, *Macromolecules*, 2010, **43**, 10201-10203; (e) R. H. Platel, A. J. P. White and C. K. Williams, *Inorg. Chem.*, 2011, **50**, 7718-7728; (f) M. Bouyahyi, N. Ajellal, E. Kirillov, C. M. Thomas and J.-F. Carpentier, *Chem. Eur. J.*, 2011, **17**, 1872-1883; (g) C. Bakewell, T. P. A. Cao, X. F. Le Goff, N. J. Long, A. Auffrant and C. K. Williams, *Organometallics*, 2013, **32**, 1475-1483; (h) K. Nie, W. Gu, Y. Yao, Y. Zhang and Q. Shen, *Organometallics*, 2013, **32**, 2608-2617; (i) N. Maudoux, T. Roisnel, J.-F. Carpentier and Y. Sarazin, *Organometallics*, 2014, **33**, 5740-5748; (j) J. S. Klitzke, T. Roisnel, E. Kirillov, O. d. L. Casagrande Jr and J.-F. Carpentier, *Organometallics*, 2014, **33**, 309-321; (k) C.-Y. Tsai, H.-C. Du, J.-C. Chang, B.-H. Huang, B.-T. Ko and C.-C. Lin, *RSC Adv.*, 2014, **4**, 14527-14537; (l) W. Gu, P. Xu, Y. Wang, Y. Yao, D. Yuan and Q. Shen, *Organometallics*, 2015, **34**, 2907-2916; (m) C. Bakewell, A. J. P. White, N. J. Long and C. K. Williams, *Inorg. Chem.*, 2015, **54**, 2204-2212; (n) T.-Q. Xu, G.-W. Yang, C. Liu and X.-B. Lu, *Macromolecules*, 2017, **50**, 515-522.
5. (a) T. P. Seifert, T. S. Brunner, T. S. Fischer, C. Barner-Kowollik and P. W. Roesky, *Organometallics*, 2018, **37**, 4481-4487; (b) H. Ma, T. P. Spaniol and J. Okuda, *Angew. Chem. Int. Ed.*, 2006, **45**, 7818-7821; (c) E. Grunova, E. Kirillov, T. Roisnel and J.-F. Carpentier, *Dalton Trans.*, 2010, **39**, 6739-6752; (d) Y. Chapurina, J. Klitzke, O. d. L. Casagrande Jr, M. Awada, V. Dorcet, E. Kirillov and J.-F. Carpentier, *Dalton Trans.*, 2014, **43**, 14322-14333; (e) H. Xie, C. Wu, D. Cui and Y. Wang, *J. Organomet. Chem.*, 2018, **875**, 5-10; (f) J. El Haj Hassan, V. Radkov, V. Dorcet, J.-F. Carpentier and E. Kirillov, *J. Organomet. Chem.*, 2016, **823**, 34-39; (g) J.-C. Buffet and J. Okuda, *Dalton Trans.*, 2011, **40**, 7748-7754; (h) Y. Cui, W. Gu, Y. Wang, B. Zhao, Y. Yao and Q. Shen, *Catal. Sci. Technol.*, 2015, **5**, 3302-3312.
6. (a) P. J. Shapiro, *Coord. Chem. Rev.*, 2002, **231**, 67-81; (b) B. Wang, *Coord. Chem. Rev.*, 2006, **250**, 242-258; (c) J. Gromada, J.-F. Carpentier and A. Mortreux, *Coord. Chem. Rev.*, 2004, **248**, 397-410.
7. W. E. Piers, P. J. Shapiro, E. E. Bunel and J. E. Bercaw, *Synlett*, 1990, **1990**, 74-84.
8. (a) P. J. Shapiro, E. Bunel, W. P. Schaefer and J. E. Bercaw, *Organometallics*, 1990, **9**, 867-869; (b) P. J. Shapiro, W. P. Schaefer, J. A. Labinger, J. E. Bercaw and W. D. Cotter, *J. Am. Chem. Soc.*, 1994, **116**, 4623-4640.
9. D. O'Hare, J. C. Green, T. Marder, S. Collins, G. Stringer, A. K. Kakkar, N. Kaltsoyannis, A. Kuhn and R. Lewis, *Organometallics*, 1992, **11**, 48-55.
10. (a) M. E. Rerek and F. Basolo, *J. Am. Chem. Soc.*, 1984, **106**, 5908-5912; (b) J. M. O'Connor and C. P. Casey, *Chem. Rev.*, 1987, **87**, 307-318; (c) M. J. Calhorda, C. C. Romão and L. F. Veiros, *Chem. Eur. J.*, 2002, **8**, 868-875.
11. M. T. Ken, T. Minoru and C. Li-Ban, *Chem. Lett.*, 1981, **10**, 729-730.
12. (a) J.-C. Buffet, T. A. Q. Arnold, Z. R. Turner, P. Angpanitcharoen and D. O'Hare, *RSC Adv.*, 2015, **5**, 87456-87464; (b) J.-C. Buffet, Z. R. Turner and D. O'Hare, *Chem. Commun.*, 2018, **54**, 10970-10973; (c) T. J. Williams, J.-C. Buffet, Z. R. Turner and D. O'Hare, *Catal. Sci. Technol.*, 2018, **8**, 5454-5461; (d) J. V. Lamb, J.-C. Buffet, Z. R. Turner and D. O'Hare, *Polym. Chem.*, 2019, **10**, 1386-1398.
13. J. V. Lamb, J.-C. Buffet, J. E. Matley, C. M. R. Wright, Z. R. Turner and D. O'Hare, *Dalton Trans.*, 2019, **48**, 2510-2520.
14. (a) J. Jenter, N. Meyer, P. W. Roesky, S. K.-H. Thiele, G. Eickerling and W. Scherer, *Chem. Eur. J.*, 2010, **16**, 5472-5480; (b) J. Jenter, G. Eickerling and P. W. Roesky, *J. Organomet. Chem.*, 2010, **695**, 2756-2760; (c) Z. Jian, W. Zhao, X. Liu, X. Chen, T. Tang and D. Cui, *Dalton Trans.*, 2010, **39**, 6871-6876; (d) J. Jenter, P. W. Roesky, N. Ajellal, S. M. Guillaume, N. Susperregui and L. Maron, *Chem. Eur. J.*, 2010, **16**, 4629-4638; (e) J. Kratsch, M. Kuzdrowska, M. Schmid, N. Kazeminejad, C. Kaub, P. Oña-Burgos, S. M. Guillaume and P. W. Roesky, *Organometallics*, 2013, **32**, 1230-1238.

15. (a) A. Kowalski, A. Duda and S. Penczek, *Macromolecules*, 1998, **31**, 2114-2122; (b) M. Save, M. Schappacher and A. Soum, *Macromol. Chem. Phys.*, 2002, **203**, 889-899.
16. R. H. Platel, L. M. Hodgson and C. K. Williams, *Polym. Rev.*, 2008, **48**, 11-63.
17. (a) A. Thevenon, C. Romain, M. S. Bennington, A. J. P. White, H. J. Davidson, S. Brooker and C. K. Williams, *Angew. Chem. Int. Ed.*, 2016, **55**, 8680-8685; (b) H.-C. Tseng, M. Y. Chiang, W.-Y. Lu, Y.-J. Chen, C.-J. Lian, Y.-H. Chen, H.-Y. Tsai, Y.-C. Lai and H.-Y. Chen, *Dalton Trans.*, 2015, **44**, 11763-11773; (c) K. Devaine-Pressing, J. H. Lehr, M. E. Pratt, L. N. Dawe, A. A. Sarjeant and C. M. Kozak, *Dalton Trans.*, 2015, **44**, 12365-12375; (d) Y. Huang, W. Wang, C.-C. Lin, M. P. Blake, L. Clark, A. D. Schwarz and P. Mountford, *Dalton Trans.*, 2013, **42**, 9313-9324.
18. A. P. Dove, V. C. Gibson, E. L. Marshall, H. S. Rzepa, A. J. P. White and D. J. Williams, *J. Am. Chem. Soc.*, 2006, **128**, 9834-9843.
19. (a) M. H. Chisholm and E. E. Delbridge, *New J. Chem.*, 2003, **27**, 1167-1176; (b) A. F. Douglas, B. O. Patrick and P. Mehrkhodavandi, *Angew. Chem. Int. Ed.*, 2008, **47**, 2290-2293.
20. P. I. Binda and E. E. Delbridge, *Dalton Trans.*, 2007, 4685-4692.
21. (a) J.-C. Wu, B.-H. Huang, M.-L. Hsueh, S.-L. Lai and C.-C. Lin, *Polymer*, 2005, **46**, 9784-9792; (b) L. Clark, G. B. Deacon, C. M. Forsyth, P. C. Junk, P. Mountford, J. P. Townley and J. Wang, *Dalton Trans.*, 2013, **42**, 9294-9312; (c) H.-Y. Chen, B.-H. Huang and C.-C. Lin, *Macromolecules*, 2005, **38**, 5400-5405.
22. T. P. A. Cao, A. Buchard, X. F. Le Goff, A. Auffrant and C. K. Williams, *Inorg. Chem.*, 2012, **51**, 2157-2169.
23. F. Bonnet, A. R. Cowley and P. Mountford, *Inorg. Chem.*, 2005, **44**, 9046-9055.
24. (a) S. M. Guillaume, M. Schappacher and A. Soum, *Macromolecules*, 2003, **36**, 54-60; (b) I. Palard, A. Soum and S. M. Guillaume, *Chem. Eur. J.*, 2004, **10**, 4054-4062; (c) R. A. Collins, J. Unruangsri and P. Mountford, *Dalton Trans.*, 2013, **42**, 759-769.
25. H. E. Dyer, S. Huijser, N. Susperregui, F. Bonnet, A. D. Schwarz, R. Duchateau, L. Maron and P. Mountford, *Organometallics*, 2010, **29**, 3602-3621.
26. (a) I. Palard, A. Soum and S. M. Guillaume, *Macromolecules*, 2005, **38**, 6888-6894; (b) G. G. Skvortsov, M. V. Yakovenko, P. M. Castro, G. K. Fukin, A. V. Cherkasov, J.-F. Carpentier and A. A. Trifonov, *Eur. J. Inorg. Chem.*, 2007, **2007**, 3260-3267.
27. N. Barros, P. Mountford, S. M. Guillaume and L. Maron, *Chem. Eur. J.*, 2008, **14**, 5507-5518.